



RELATIVE ROLES OF CLOUD, RADIATIVE, AND SOLAR-GEOMAGNETIC PROCESSES IN MODULATING CONVECTIVE AVAILABLE POTENTIAL ENERGY ACROSS NIGERIAN CLIMATE ZONES

*¹Grace ADAGBA, ²Tertsea IGBAWUA, and ²Emmanuel Vezua TIKYAA

¹Moses Orshio Adasu University, Makurdi, Benue State, Nigeria.

²Joseph Sarwuan Tarka University, Makurdi, Benue State, Nigeria.

*Correspondence authors' email: domgrace1@gmail.com Phone: +2347082130006

Abstract

This study examines the effects of cloud properties, solar thermal radiation, and solar-geomagnetic indices on convective available potential energy (CAPE) across Nigeria's tropical rainforest (Af), tropical monsoon (Am), and tropical savanna (Aw) climate zones from 1994 to 2024. Daily reanalysis and satellite-derived datasets were aggregated into climatological means. Statistical relationships were analyzed using lag-correlation and Normalized information flow (NIF), based on transfer entropy, was used to quantify directional causal influence among variables to quantify directional influences among variables. Mean CAPE values are highest in the Af and Am zones, frequently exceeding 2000–3000 J kg⁻¹ during peak convective periods, while the Aw zone exhibits lower and more seasonal CAPE, typically ranging from 500 to 1800 J kg⁻¹. Cloud fraction remains persistently high in the Af and Am zones (>0.60), coinciding with enhanced convective precipitation (CONPRE) and pronounced CAPE variability. Solar thermal radiation downward (STRD) contributes indirectly through surface heating, with shortwave fluxes of approximately 220–260 W m⁻² during the dry season, particularly influencing CAPE in the Aw zone. In contrast, solar and geomagnetic indices, including F10.7obs (FL) and Ap, show low mean values and weak correlations with CAPE. Information flow analysis indicates that cloud and precipitation processes account for more than 60% of CAPE variability, whereas solar and geomagnetic parameters contribute less than 10%. Collectively, CAPE variability across Nigeria is dominated by internal atmospheric processes, with limited direct modulation by external solar-geomagnetic forcing

Keywords: Convective available potential energy (CAPE); Cloud fraction; Solar thermal radiation downward; Solar activity; Geomagnetic indices; Climate zones; Nigeria

1. Introduction

Thunderstorms are a predominant atmospheric phenomenon in the tropics, producing intense rainfall, lightning, strong winds, and flooding, all of which have significant socio-economic and environmental impacts. In tropical and subtropical regions, convective storms contribute a large portion of the annual precipitation and drive hydrological extremes (de Coning et al., 2011; Pinto and Belo-Pereira, 2020; Jelić et al., 2021). These hazards are primarily associated with deep convective clouds, particularly cumulonimbus systems (Groenemeijer et al., 2014; Matsui et al., 2020).

Atmospheric instability is a fundamental prerequisite for the development of convective storms and is commonly quantified using thermodynamic indices such as convective available potential energy (CAPE), convective inhibition (CIN), the lifted index (LI), the K-index (KI), and the total totals index (TTI) (Galway, 1956; DeRubertis, 2006). While these indices are widely used in forecasting and climatological studies, their effectiveness varies significantly across different climatic regimes, particularly between mid-latitude and tropical environments (Sun et al., 2019; Fernando et al., 2021).

In tropical regions, high CAPE does not necessarily result in deep convection, underscoring the regulatory roles of cloud formation, precipitation, and moisture redistribution under near-convective quasi-equilibrium conditions (Xu and Emanuel, 1989; Louf et al., 2019). Consequently, cloud structure, radiative feedbacks, entrainment, and large-scale dynamics significantly influence whether the available instability is released as convection (Igel et al., 2015; Emanuel, 2023). Recent studies have increasingly emphasized that cloud–precipitation interactions can dominate convective energetics and often provide greater explanatory power than CAPE alone (Jelić et al., 2021).

Over West Africa, where mesoscale convective systems dominate rainfall variability and extreme weather, most existing studies have examined CAPE either in isolation or alongside traditional thermodynamic indices. However, there have been limited efforts to quantify the directional and relative contributions of cloud processes to CAPE variability using causal or information-theoretic approaches (de Coning et al., 2011; Mathew et al., 2021). Furthermore, despite increasing recognition of the importance of cloud–radiation

interactions in tropical convection, their explicit role in modulating CAPE across distinct West African climate zones remains insufficiently quantified. This gap is largely due to observational constraints and the scarcity of integrative multi-source analyses (Ashidi *et al.*, 2024).

In addition to internal atmospheric controls, solar thermal radiation and solar-geomagnetic variability have been proposed as potential external modulators of atmospheric circulation, cloud microphysics, and precipitation. Although previous studies suggest that solar and geomagnetic activity exert weaker influences on convective instability compared to internal thermodynamic and cloud processes, reported correlations between solar variability, cloud cover, and rainfall warrant a systematic assessment of their potential indirect effects on CAPE, particularly in data-sparse tropical regions (Adu and Okeke, 2019; Hanson *et al.*, 2021). Evaluating these forcings alongside dominant atmospheric controls enables a quantitative determination of their relative importance, thereby avoiding implicit assumptions about their insignificance and clarifying whether their influence is negligible, secondary, or regime-dependent.

Previous studies over West Africa have primarily examined CAPE in isolation or alongside traditional thermodynamic indices, with few efforts to quantify the directional and relative contributions of cloud processes and external solar-geomagnetic forcing using causal metrics.

Against this backdrop, this study examines the effects of cloud properties, solar thermal radiation, and solar-geomagnetic indices on CAPE across Nigeria's Af, Am, and Aw climate zones during 1994–2024. By integrating multi-source satellite and reanalysis datasets and applying information flow and lag-correlation analyses, the study explicitly quantifies the directional and relative contributions of internal atmospheric processes and external forcing to convective instability. This approach addresses a critical gap in existing West African convection research and advances the understanding of the mechanisms regulating tropical instability across contrasting climate regimes.

2. Methodology

2.1 Study Area and Climate Zonation

The study focuses solely on Nigeria's Af (tropical rainforest), Am (tropical monsoon), and Aw (tropical savanna) climate zones, as these regions provide the most complete and consistent CAPE datasets necessary for robust analysis. Other climate zones within Nigeria were excluded due to substantial gaps or missing values in the CAPE records, which could compromise the reliability and statistical validity of the results. By concentrating on these three zones, the study ensures a comprehensive assessment of convective instability across regions with distinct moisture regimes, cloud structures, and convective dynamics, allowing for meaningful comparisons of

daily variations in atmospheric instability. This approach maximizes data integrity and also demonstrates the contrasting influences of cloud properties, solar radiation, and geomagnetic activity on CAPE across Nigeria's principal tropical climate regimes. The Köppen climate classifications are shown in Figure 1.

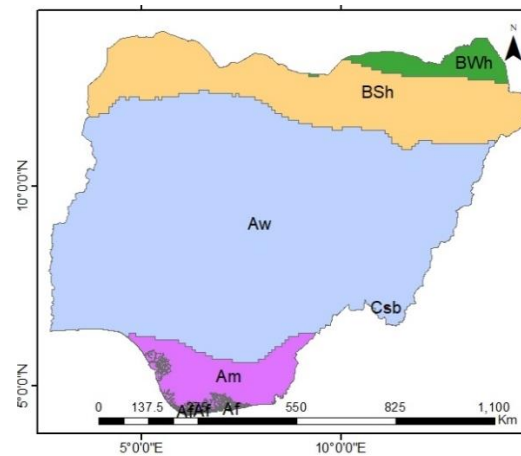


Figure 1 Study Area

2.2 Data Sources

Daily convective available potential energy (CAPE), cloud fraction (Total cloud cover (TCC), High cloud cover (HCC), Midum ciud cover (MCC), and Low cloud cover cover (LCC)), CONPRE, and STRD were obtained from reanalysis and satellite-derived datasets for the period 1994–2024 from the European Centre for Medium-Range Weather Forecasts (ECMWF) Reanalysis Version 5 (ERA5). Solar and geomagnetic indices, sourced from <https://kp.gfz.de/en/data>, were characterized using standard indices, including sunspot number (SN), F10.7obs, which is the 10.7-cm solar radio flux (FL) at 10.7 cm, planetary geomagnetic K-index (Kp), and the geomagnetic activity index (Ap). The spatial resolution of the ERA5 datasets is given as $0.25^\circ \times 0.25^\circ$.

2.3 Data Processing and Analysis

Daily data were initially processed from hourly values to generate daily climatologies, enabling visualization of temporal patterns and variability in CAPE and the explanatory variables across the three climate zones (Af, Am, and Aw) from 1994 to 2024. To ensure regional representativeness, spatial averaging was performed within each Köppen zone. The target variable, CAPE, along with predictor variables—including cloud fractions, CONPRE, STRD, and solar geomagnetic indices, were analyzed. Minor gaps in the dataset were appropriately handled using interpolation techniques. COPRE and STRD

Temporal relationships between CAPE and its predictors were assessed using lag-correlation analysis with up to five daily lags to capture time-delayed interactions. To quantify the relative and directional influences of each predictor on CAPE,

normalized information flow (NIF) analysis was employed. The NIF method evaluates causal information transfer between time series while accounting for nonlinear interactions and feedback mechanisms, expressing the result as a percentage of the total information flow to the target variable. Following Zeng *et al.* (2022), effective transfer entropy was interpreted as information flow and normalized to obtain the normalized information flow. This method has been successfully applied in climate studies by Hu *et al.* (2022), Stips *et al.* (2016), and Liang *et al.* (2016). For multivariate attribution, the information flow from each predictor was further normalized by the total effective information flow into the target. The NIF equation used is:

$$NIF_{X \rightarrow Y} = \frac{K_{X \rightarrow Y}}{H(Y)} \times 100$$

where $K_{X \rightarrow Y}$ represents the effective transfer entropy (TE_{eff}) and $H(Y) = -\sum_j p(y) \ln p(y)$ is the Shannon entropy of the target Y. This approach enabled the identification of the dominant drivers of convective instability in each climate zone, accounting for both cloud–radiation interactions and external solar–geomagnetic forcings.

2.4 Statistical Significance

Statistical significance of correlations and information flow estimates was assessed using confidence intervals and surrogate data testing, with a significance threshold set at $p < 0.05$. This approach ensured that the identified relationships were robust and not due to random variability.

3 Results

3.1 Descriptive Statistics for the Variables across the Climate zones

Table 1 presents the descriptive statistics of key atmospheric and cloud-related variables across the three Köppen climate zones (Af, Am, and Aw), showing clear spatial contrasts in convective conditions, precipitation, cloud structure, and radiative fluxes.

The results indicate that the Af climate exhibits the most intense convective and radiative environment. CAPE values are highest in the Af climate, with a mean of approximately 869 J/kg and a maximum nearing 2900 J/kg, signifying strong atmospheric instability conducive to deep convection. This finding aligns with established climatological interpretations, which associate persistent moisture availability and elevated surface temperatures with enhanced convective potential in equatorial rainforest regions. The Af climate also records relatively high mean convective precipitation (18.48 mm/day) and the highest mean total cloud cover (TCC ≈ 0.78), reflecting frequent and extensive cloud formation. Additionally, the elevated mean STRD values suggest strong

surface downwelling longwave radiation, likely linked to dense cloud cover and high atmospheric moisture content.

The Am climate exhibits characteristics broadly similar to those of the Af climate but with slightly reduced intensity. Mean CAPE (≈ 813 J/kg) and precipitation (≈ 20.02 mm/day) remain high, reflecting the strong seasonal influence of monsoonal circulation. Cloud fractions in Am are comparable to those in Af, with a slightly higher mean TCC (approximately 0.80), indicating persistent cloudiness during the wet season. However, marginally lower HCC and MCC values suggest some vertical redistribution of cloud layers compared to Af. Surface thermal radiation downwards (STRD) values in Am are also high and comparable to those in Af, reinforcing the role of cloud cover and humidity in enhancing downward longwave radiation.

In contrast, the Aw (tropical savanna) climate exhibits significantly weaker convective activity and cloud characteristics. The mean CAPE decreases to approximately 543 J/kg, and mean precipitation declines sharply to 8.75 mm/day, reflecting the pronounced seasonal dryness typical of savanna regions. Cloud cover fractions (HCC, MCC, LCC, and TCC) are consistently lower in Aw compared to Af and Am climates, with the mean TCC around 0.63. This reduced cloudiness corresponds to greater surface exposure to radiative cooling at night and more pronounced seasonal variability. STRD values in Aw are also lower on average, consistent with reduced atmospheric moisture and diminished cloud insulation.

Comparatively, Af and Am climates are characterized by strong convection, high cloud cover, and elevated radiative fluxes, whereas Aw represents a transition toward drier and less energetically active atmospheric conditions. These differences highlight the significant influence of climate regimes on cloud structure, convective energy, and surface radiation, consistent with established World Meteorological Organization (WMO) (Canton, 2021) climatological frameworks that associate tropical climate zones with variations in atmospheric stability and hydrometeorological behavior.

Table 2 presents the descriptive statistics of solar and geomagnetic parameters, showing generally low average activity with intermittent extreme events. The Ap index ranges from 0.00 to 271.00, with a mean of 10.26 ± 12.13 , indicating mostly quiet geomagnetic conditions punctuated by strong disturbances. The sunspot number varies widely between 0.00 and 353.00, with a mean of 65.83 and a standard deviation of 63.32, reflecting significant solar cycle variability. The F10.7obs values span from 53.50 to 938.60, averaging 109.58 ± 45.56 , suggesting alternating periods of weak and enhanced solar radiative output. Kp values range from 0.00 to 8.38, with a mean of 1.83 ± 1.11 , indicating predominantly low geomagnetic activity with occasional storms.

Table 1 Descriptive Statistics for the Variables across the Climate zones

Koppen Climate	Variable	CAPE (J/kg)	CONPRE (mm/day)	HCC	MCC	LCC	TCC	STRD (J/m ²)
Af	min	0.00	0.00	0.00	0.00	0.00	0.00	1255373.84
	max	2896.55	143.20	1.00	1.00	1.00	1.00	1587294.64
	mean	868.56	18.48	0.66	0.26	0.34	0.78	1517928.24
	sd	563.98	16.29	0.28	0.19	0.17	0.22	29331.25
Variable	CAPE	CONPRE	HCC	MCC	LCC	TCC	STRD	
Am	min	0.00	0.00	0.00	0.00	0.00	0.01	1225960.03
	max	2722.29	97.50	1.00	0.97	0.98	1.00	1592429.47
	mean	812.75	20.02	0.66	0.25	0.38	0.80	1511238.47
	sd	490.72	16.06	0.27	0.17	0.16	0.20	34207.02
Variable	CAPE	CONPRE	HCC	MCC	LCC	TCC	STRD	
Aw	min	0.00	0.00	0.00	0.00	0.00	0.00	1089036.04
	max	1979.43	65.23	0.99	0.87	0.84	1.00	1570546.04
	mean	543.32	8.75	0.53	0.16	0.20	0.63	1419897.64
	sd	382.72	9.84	0.25	0.14	0.15	0.25	99223.33

Table 2 Descriptive Statistics for the solar and geomagnetic parameters

Variable	Ap	SN	F10.7obs	Kp
min	0.00	0.00	53.500	0.00
max	271.00	353.00	938.60	8.38
mean	10.26	65.83	109.579	1.83
sd	12.13	63.32	45.559	1.11

3.2 Daily Climatology of CAPE, Solar and Geomagnetic parameters

Figure 2 illustrates the daily climatology of CAPE across the Af, Am, and Aw climate zones, averaged over 1994–2024, revealing distinct seasonal patterns and contrasts among the zones. In the Af climate, CAPE rises sharply at the beginning of the year, reaching a peak of approximately 1750 J/kg around day 90, before gradually declining to a minimum below 200 J/kg near mid-year. A secondary increase occurs toward the end of the year, reflecting persistent convective activity typical of equatorial rainforest regions. The Am (tropical monsoon) climate exhibits a slightly lower peak of around 1500 J/kg near day 80, followed by a pronounced mid-year minimum below 200 J/kg, indicating strong seasonal modulation driven by monsoonal circulation. CAPE gradually recovers toward the end of the year, showing a secondary maximum slightly above 1000 J/kg.

In contrast, the Aw climate exhibits a bimodal CAPE pattern, with two distinct peaks: the first around 1,050 J/kg near day 150 and the second approximately 1,100 J/kg near day 270, separated by a pronounced mid-year minimum below 100 J/kg. This bimodality reflects the seasonal wet and dry cycles

typical of savanna climates, characterized by reduced convection during the dry season. Across all zones, variability, indicated by the shaded regions, is greatest during peak CAPE periods, suggesting higher day-to-day fluctuations in atmospheric instability. Generally, Af and Am climates maintain consistently higher CAPE values throughout the year, indicating stronger and more sustained convective potential, whereas Aw exhibits more pronounced seasonal variability and lower mean convective energy. These patterns underscore the significant influence of climate regime on atmospheric instability and the timing of convective activity.

Figure 3 presents the daily climatology of solar and geomagnetic parameters averaged from 1994 to 2024. Ap values mostly range between 10 and 20, indicating generally low geomagnetic activity, although occasional spikes exceed 25. The observed F10.7 flux remains stable around 120 solar flux units, with minor increases above 150 during periods of heightened solar activity. The Kp index fluctuates near 2, reflecting mild geomagnetic disturbances, while short-term peaks surpass 3. The sunspot number (SN) averages around 60 and shows variability linked to the solar cycle, with

occasional maxima approaching 120. Broadly, the data indicate a generally low baseline for both geomagnetic and solar parameters, punctuated by episodic events. These variations suggest periods of enhanced solar and geomagnetic influence that could impact near-Earth space weather conditions.

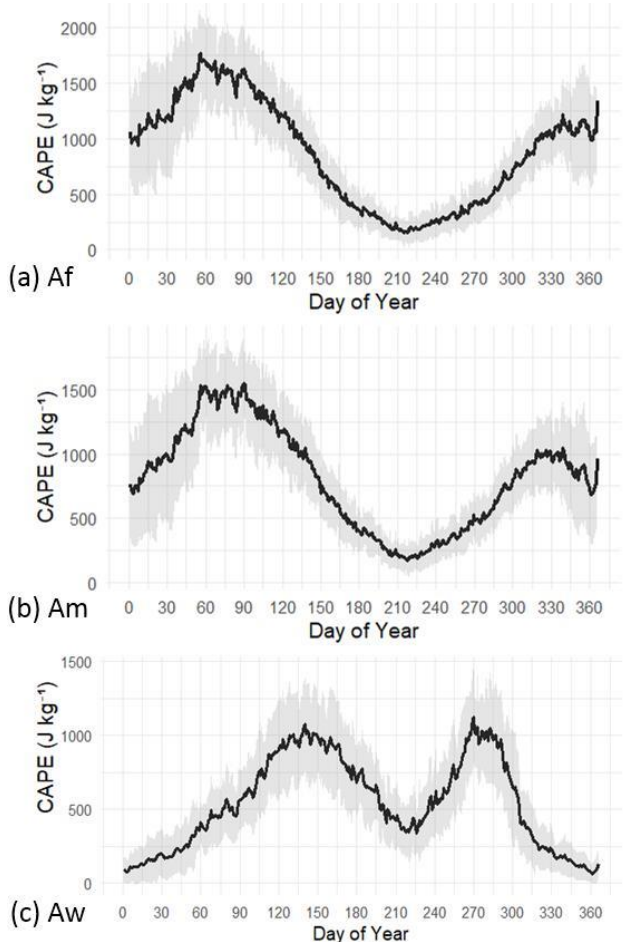


Figure 2 Daily Climatology of CAPE across the climate zones averaged from 1994 to 2024

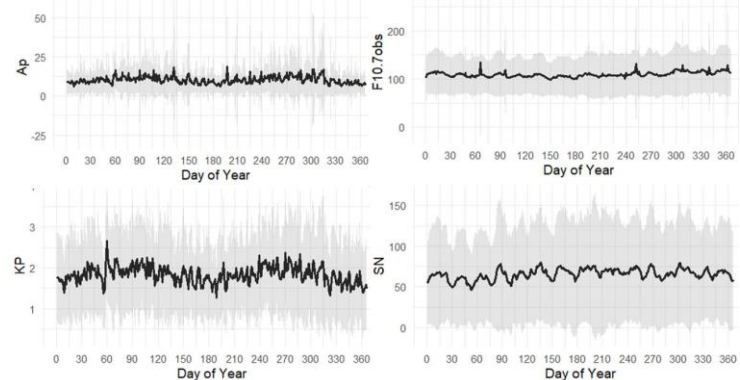


Figure 3 Daily Climatology of Solar and Geomagnetic parameters averaged from 1994 to 2024

3.3 Normalized Information Flow between CAPE and CONPRE, Cloud parameters, Solar and Geomagnetic Parameters

Table 3 shows that cloud-related variables exert the strongest control on CAPE in the Af zone, as indicated by consistently

high NIF values and strong statistical significance. In the X→Y direction, CONPRE, TCC, MCC, and LCC demonstrate very strong information transfer to CAPE (NIF = 0.944, $p < 0.001$), revealing precipitation–cloud dominance. HCC also contributes significantly, though moderately, with an NIF of 0.750 ($p = 0.02$), suggesting that vertical cloud structure influences CAPE variability. Solar–geomagnetic drivers have a secondary influence; FL exhibits high coupling with CAPE (NIF = 0.900, $p < 0.001$), while Ap and Kp show moderately significant effects (NIF = 0.600–0.750). The sunspot number shows negligible influence on CAPE in this direction (NIF = 0.000, $p = 0.68$), indicating minimal direct modulation by solar-cycle variability rather than seasonal forcing.

In the reverse Y→X direction, CAPE feeds back significantly to CONPRE and TCC (NIF = 0.778–0.923, $p < 0.001$), confirming bidirectional coupling. Feedback from cloud layers weakens progressively from HCC to LCC (NIF = 0.714–0.750, $p = 0.02$), reflecting stratified atmospheric responses. Geomagnetic feedback persists through Ap and Kp indices (NIF = 0.600–0.800, $p \leq 0.02$), but solar influence weakens substantially. FL becomes insignificant in the reverse direction (NIF = 0.500, $p = 0.16$), while SN remains consistently negligible ($p > 0.20$). Generally, CAPE dynamics in the Af zone are primarily governed by cloud–precipitation interactions, with solar and geomagnetic effects acting as weaker, direction-dependent modulators.

Table 3 also indicates a very strong cloud–precipitation control on CAPE in the Am zone, with CONPRE exhibiting dominant bidirectional information flow (NIF = 0.961–0.983, $p < 0.001$). In the X→Y direction, MCC and LCC strongly influence CAPE, with NIF values of 0.946 and 0.950, respectively, both highly significant ($p < 0.001$). TCC shows moderate but significant coupling with CAPE (NIF = 0.833, $p = 0.01$), whereas HCC influence is weak and statistically insignificant (NIF = 0.500, $p = 0.20$). Geomagnetic forcing is limited: Kp shows a moderately significant influence (NIF = 0.714, $p < 0.001$), while Ap exhibits no meaningful coupling (NIF = 0.000, $p = 0.39$). Solar parameters contribute weakly, with FL insignificant (NIF = 0.500, $p = 0.19$) and SN showing no influence (NIF = 0.000, $p = 0.71$).

In the reverse Y→X direction, CAPE strongly feeds back to cloud parameters, particularly LCC (NIF = 0.988, $p < 0.001$) and MCC (NIF = 0.964, $p < 0.001$). TCC and HCC also exhibit significant feedback on CAPE variability (NIF = 0.962 and 0.800, respectively, $p < 0.001$), indicating enhanced bidirectional coupling. Geomagnetic feedback weakens, as Ap remains marginally significant (NIF = 0.500, $p = 0.01$), while Kp becomes insignificant (NIF = 0.333, $p = 0.12$). These results suggest that CAPE dynamics in the Am zone are predominantly governed by cloud and precipitation processes, with solar and geomagnetic influences remaining weak and inconsistent.

In the Aw climate zone, cloud and precipitation exert a strong control on CAPE, with CONPRE and TCC demonstrating near-unity information flow (NIF = 0.986–0.993, $p < 0.001$), as shown in Table 3. In the X→Y direction, MCC and LCC significantly influence CAPE, with NIF values of 0.981 and 0.980, respectively, both highly significant ($p < 0.001$). HCC also exhibits strong coupling with CAPE (NIF = 0.962, $p < 0.001$), indicating a robust role of vertical cloud structure. Solar and geomagnetic drivers are negligible in this direction: Ap shows zero information flow ($p = 0.28$), while Kp and FL remain weak and insignificant ($p > 0.20$). The sunspot number shows no detectable influence on CAPE (NIF = 0.000, $p = 0.77$), confirming minimal solar-cycle control.

In the reverse Y→X direction, CAPE exhibits a strong feedback effect on cloud and precipitation variables, particularly LCC (NIF = 0.990, $p < 0.001$) and CONPRE (NIF = 0.993, $p < 0.001$). TCC, HCC, and MCC also demonstrate near-complete feedback coupling with CAPE (NIF = 0.982–0.993, $p < 0.001$), indicating a robust bidirectional dependence. Solar forcing is marginally relevant only through FL (NIF = 0.833, $p = 0.02$), while Ap, Kp, and SN remain statistically insignificant. Collectively, CAPE variability in the Aw zone is predominantly governed by cloud and precipitation processes, with solar and geomagnetic influences being largely negligible and direction-specific.

Table 3 Normalized Information Flow between CAPE and others variables

X-Y		Y-X				
Variable	NIF	p-value	Variable	NIF	p-value	
Af	CONPRE	0.944	0.0000	CONPRE	0.778	0.0000
	TCC	0.944	0.0000	TCC	0.923	0.0000
	HCC	0.750	0.0200	HCC	0.750	0.0200
	MCC	0.944	0.0000	MCC	0.750	0.0200
	LCC	0.944	0.0000	LCC	0.714	0.0200
	Ap	0.600	0.0200	Ap	0.800	0.0000
	Kp	0.750	0.0200	Kp	0.600	0.0200
	FL	0.900	0.0000	FL	0.500	0.1600
	SN	0.000	0.6800	SN	0.000	0.2300
Am	Variable	NIF	p-value	Variable	NIF	p-value
	CONPRE	0.961	0.0000	CONPRE	0.983	0.0000
	TCC	0.833	0.0100	TCC	0.962	0.0000
	HCC	0.500	0.2000	HCC	0.800	0.0000
	MCC	0.946	0.0000	MCC	0.964	0.0000
	LCC	0.950	0.0000	LCC	0.988	0.0000
	Ap	0.000	0.3900	Ap	0.500	0.0100
	Kp	0.714	0.0000	Kp	0.333	0.1200
	FL	0.500	0.1900	FL	0.500	0.1900
Aw	SN	0.000	0.7100	SN	0.000	0.7100
	Variable	NIF	p-value	Variable	NIF	p-value
	CONPRE	0.986	0.0000	CONPRE	0.993	0.0000
	TCC	0.987	0.0000	TCC	0.993	0.0000
	HCC	0.962	0.0000	HCC	0.986	0.0000
	MCC	0.981	0.0000	MCC	0.982	0.0000
	LCC	0.980	0.0000	LCC	0.990	0.0000
	Ap	0.000	0.2800	Ap	0.000	0.6000
	Kp	0.500	0.2400	Kp	0.000	0.8400
	FL	0.500	0.2200	FL	0.833	0.0200
	SN	0.000	0.7700	SN	0.333	0.0900

3.3 Lag correlation plot between CAPE and Cloud, CONPRE, Solar and Geomagnetic parameters across the climate zones from 1994 to 2024

Figure 4 shows that in the Af zone, cloud parameters predominantly influence CAPE variability. STRD exhibits the strongest positive correlation at zero lag (~ 0.25), which gradually weakens as the lag increases. TCC and CONPRE in the Af zone maintain persistent negative correlations with CAPE (approximately -0.20 to -0.25), indicating sustained inverse cloud–instability relationships across lags of 0 to 5 days. LCC and MCC in the Af zone display strong negative correlations near zero lag (around -0.50), remaining relatively stable with increasing lag, highlighting the suppression of CAPE by low-level clouds. Solar and geomagnetic parameters in the Af zone, including Ap, Kp, SN, and F10.7, cluster near zero correlation, suggesting minimal lagged influence on CAPE.

In the Am zone, most variables exhibit weak correlations with CAPE across all lags, indicating a reduced sensitivity of atmospheric instability to external forcing. MCC in the Am zone shows a notable negative correlation at zero lag (approximately -0.45), but this effect rapidly diminishes, suggesting a short-lived cloud modulation of CAPE. STRD maintains a small positive correlation (around 0.30) at zero lag in the Am zone, though its lagged persistence is limited.

In the Aw zone, cloud parameters exhibit strong instantaneous coupling with CAPE, with STRD showing a very high positive correlation at zero lag (~ 0.70). HCC, MCC, and LCC in the Aw zone display moderate positive correlations at zero lag (approximately 0.25–0.45), but these correlations sharply decline beyond one day. Solar and geomagnetic indices across the Aw zone remain near zero or weakly negative, confirming negligible delayed influence on CAPE.

Generally, Figure 4 indicates that CAPE primarily responds to cloud and precipitation processes at short time scales, with limited lagged influence from solar and geomagnetic forcing across all climate zones.

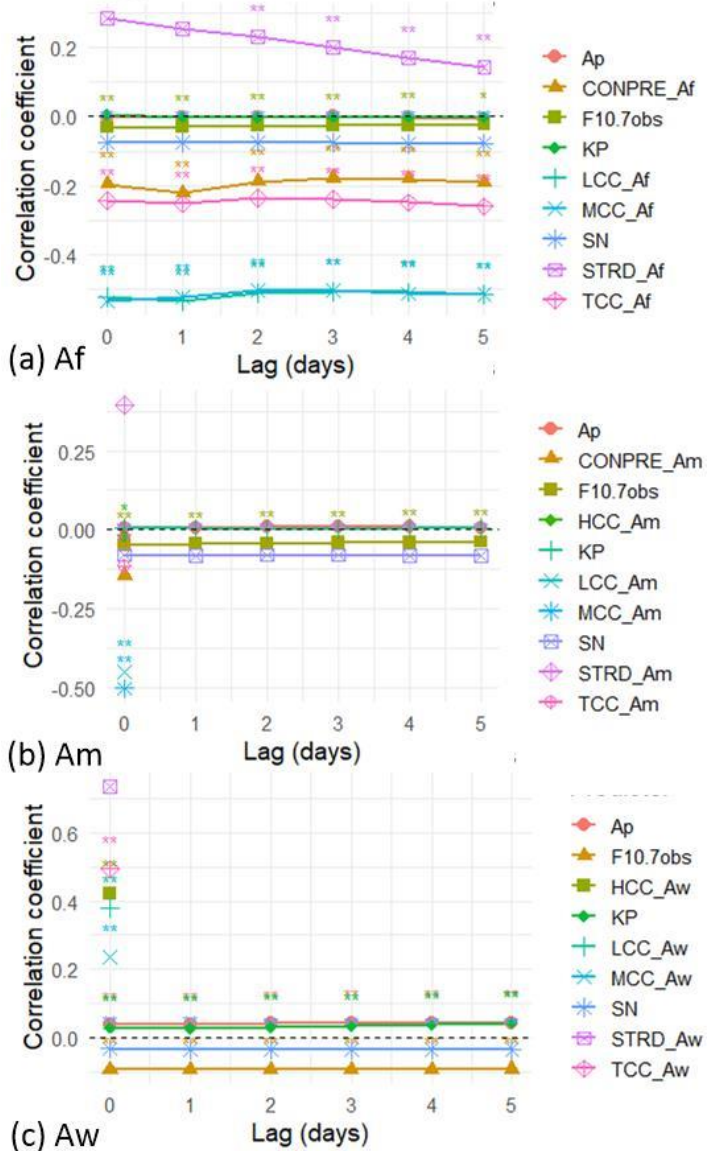


Figure 4 Lag correlation plot between CAPE and Cloud, CONPRE, Solar and Geomagnetic parameters across the climate zones from 1994 to 2024

4 Discussion

The observed dominance of cloud and precipitation variables in modulating CAPE across the Af, Am, and Aw climate zones is strongly supported by previous convective climatology studies. In the Af and Am zones, persistently high CAPE, cloud fractions, and convective precipitation reflect thermodynamic environments characteristic of deep tropical convection, where moisture availability and cloud-radiation feedbacks sustain atmospheric instability (de Coning *et al.*, 2011; Mathew *et al.*, 2021; Ashidi *et al.*, 2024). Consistent with findings from other tropical regions, CAPE in these zones exhibits strong bidirectional coupling with cloud layers, particularly middle and low cloud cover, emphasizing the role of cloud microphysics and moisture recycling rather than isolated thermodynamic instability alone (Fernando *et al.*, 2021; Igel *et al.*, 2015). This aligns with Emanuel (2023), who

demonstrated that CAPE accumulation over land is strongly influenced by surface moisture, vegetation, and boundary-layer evolution rather than solely by large-scale forcing.

The comparatively weaker CAPE and stronger seasonality observed in the Aw climate zone reflect savanna-type convection, where instability is episodic and tightly constrained by cloud development and precipitation processes. The near-unity normalized information flow among CAPE, convective precipitation, and cloud parameters in the Aw zone confirms that convective feedbacks dominate instability regulation. This finding is consistent with studies showing that tropical convection often operates near quasi-equilibrium conditions despite moderate CAPE values (Xu and Emanuel, 1989; Louf *et al.*, 2019).

The consistently weak influence of solar and geomagnetic parameters across all climate zones can be attributed to a fundamental energy-scale mismatch and the indirect nature of solar-geomagnetic pathways. Variability in solar and geomagnetic indices primarily affects the upper atmosphere and ionosphere, whereas CAPE is governed by lower-tropospheric thermodynamics, moisture availability, and cloud microphysical processes. Any potential solar-geomagnetic influence on convection therefore occurs indirectly, through the slow modulation of circulation patterns or cloud nucleation processes, and is easily overshadowed by the magnitude and immediacy of internal atmospheric feedbacks in the tropics. This interpretation aligns with previous studies in West Africa and Nigeria, which report that solar magnetic activity exerts, at most, weak and indirect influences on weather variability compared to dominant thermodynamic and cloud-driven processes (Hanson *et al.*, 2021; Audu and Okeke, 2019; Oloketuyi and Omole, 2024).

Furthermore, the weak standalone influence of CAPE on convective intensity aligns with both tropical and global-scale studies indicating that CAPE alone is often insufficient for predicting thunderstorm occurrence or severity (DeRubertis, 2006; Sun *et al.*, 2019; Peters *et al.*, 2024). Instead, cloud structure, moisture stratification, and entrainment govern how available energy is realized as convection, particularly in warm, humid environments where dilution effects are pronounced (Früh and Wirth, 2007; Igel *et al.*, 2015; Peters *et al.*, 2024). These findings reinforce the need for integrated diagnostic frameworks that combine CAPE with cloud and precipitation metrics, as demonstrated by composite instability indices and lightning-based diagnostics (Jelić *et al.*, 2021; Galway, 1956).

A key limitation of this study stems from the use of gridded reanalysis and satellite-derived datasets, which inherently smooth small-scale variability and may artificially inflate apparent coupling among closely related atmospheric variables. Consequently, the near-unity NIF values ($\approx 0.98-0.99$) observed between CAPE, cloud fractions, and convective precipitation likely reflect strong physical co-

dependence and feedbacks within convective systems, as well as redundancy introduced by shared retrieval algorithms and spatial averaging, rather than independent causal forcing. Cloud development, precipitation, and CAPE co-evolve through tightly linked thermodynamic and microphysical processes, and their representation on a common grid can enhance mutual information content. Additionally, uncertainties associated with cloud parameter retrievals, limited vertical resolution, and the inability of reanalysis products to fully resolve mesoscale convective processes may affect the magnitude of inferred information flow. Finally, while effective transfer entropy reduces bias from autocorrelation and finite sample sizes, it remains sensitive to data length, temporal resolution, and binning choices, which should be considered when interpreting causality strength rather than direction.

Conclusion

This study evaluated the influence of cloud properties, solar thermal radiation, and solar-geomagnetic indices on convective available potential energy (CAPE) across Nigeria's Af, Am, and Aw climate zones from 1994 to 2024. The results indicate that CAPE variability is primarily driven by internal atmospheric processes, especially cloud fraction and convective precipitation, which show strong and consistent correlations with atmospheric instability across all climate zones. The Af and Am regions exhibit persistently high CAPE linked to sustained cloud development and moisture availability, whereas the Aw zone demonstrates lower and more seasonally variable CAPE, characteristic of savanna-type convection.

Solar thermal radiation indirectly influences CAPE variability by heating the surface and destabilizing the boundary layer, with a more pronounced effect in the Aw climate zone during dry-season conditions. In contrast, solar and geomagnetic indices, such as F10.7obs and Ap, exhibit weak and inconsistent correlations with CAPE, suggesting limited direct modulation of convective instability by external solar-geomagnetic forcing. Information-flow analysis confirms that cloud and precipitation processes account for the majority of CAPE variability, while solar and geomagnetic influences remain marginal.

In general, the findings emphasize the primary role of cloud-precipitation feedbacks in regulating tropical atmospheric instability over Nigeria and highlight the limited influence of solar-geomagnetic forcing. Future research could incorporate vertical thermodynamic profiles and aerosol-cloud interactions to better constrain convective instability diagnostics and enhance the representation of mesoscale convective processes in tropical environments.

Declaration

The authors declare no conflict of interest

References

Ashidi, A. G., Kareem, A. I., Alade, O., & Omitusa, O. (2024). Analysis of atmospheric stability and convective activities for radio applications over selected locations in Nigeria. *The Journal of the Nigerian Association of Mathematical Physics*, 67(1), 93–104.

Audu, M. O., & Okeke, F. N. (2019). Investigation of possible connections between solar activity and climate change in Nigeria. *SN Applied Sciences*, 1(2), 149 <https://doi.org/10.1007/s42452-019-0160-x>

Canion, H. (2021). World meteorological organization—WMO. In *The Europa directory of international organizations 2021* (pp. 388–393). Routledge.

de Coning, E., Koenig, M., & Olivier, J. (2011). The combined instability index: A new very-short-range convection forecasting technique for southern Africa. *Meteorological Applications*, 18(4), 421–439. <https://doi.org/10.1002/met.234>

DeMott, C. A., & Randall, D. A. (2004). Observed variations of tropical convective available potential energy. *Journal of Geophysical Research: Atmospheres*, 109(D2). <https://doi.org/10.1029/2003JD004127>

DeRubertis, D. (2006). Recent trends in four common stability indices derived from U.S. radiosonde observations. *Journal of Climate*, 19(3), 309–323. <https://doi.org/10.1175/JCLI3622.1>

Dergachev, V. A., Vasiliev, S. S., & Raspovov, O. M. (2012). Impact of the geomagnetic field and solar radiation on climate change. *Geomagnetism and Aeronomy*, 52, 959–976. <https://doi.org/10.1134/S0016793212080063>

Emanuel, K. (2023). On the physics of high CAPE. *Journal of the Atmospheric Sciences*, 80(11), 2669–2683. <https://doi.org/10.1175/JAS-D-23-0024.1>

Fernando, M., Millangoda, M., & Premalal, S. (2021). Analysis and comparison of atmospheric instability using K-index, lifted index, total totals index, CAPE, and CIN during thunderstorm development in Sri Lanka. In D. Amaralunga, R. Haigh, & N. Dias (Eds.), *Multi-hazard early warning and disaster risks* (pp. 603–614). Springer. https://doi.org/10.1007/978-3-030-73003-1_41

Früh, B., & Wirth, V. (2007). Convective available potential energy (CAPE) in mixed-phase cloud conditions. *Quarterly Journal of the Royal Meteorological Society*, 133(624), 561–569. <https://doi.org/10.1002/qj.45>

Galway, J. G. (1956). The lifted index as a predictor of latent instability. *Bulletin of the American Meteorological Society*, 37, 528–529.

Groenemeijer, P., & Kühne, T. (2014). A climatology of tornadoes in Europe: Results from the European Severe Weather Database. *Monthly Weather Review*, 142, 4775–4790. <https://doi.org/10.1175/MWR-D-14-00107.1>

Hanson, E. A., & Okeke, F. N. (2021). Impacts of sunspot number and geomagnetic aa-index on climate of wet

zone West Africa during solar cycles 22–24. *Scientific Reports*, 11, 11500. <https://doi.org/10.1038/s41598-021-90999-6>

Hu, H., Tan, Z., Liu, C., Wang, Z., Cai, X., Wang, X., Ye, Z. & Zheng, S. (2022) Multi-timescale analysis of air pollution spreaders in Chinese cities based on a transfer entropy network. *Front. Environ. Sci.* 10:970267. <https://doi.org/10.3389/fenvs.2022.970267>

Igel, M. R., & van den Heever, S. C. (2015). The relative influence of environmental characteristics on tropical deep convective morphology as observed by CloudSat. *Journal of Geophysical Research: Atmospheres*, 120(9), 4304–4322. <https://doi.org/10.1002/2014JD022690>

Jelić, D., Telišman Prtenjak, M., Malečić, B., Belušić Vozila, A., Megyeri, O. A., & Renko, T. (2021). A new approach for the analysis of deep convective events: Thunderstorm intensity index. *Atmosphere*, 12(7), 908. <https://doi.org/10.3390/atmos12070908>

Liang, X. S. (2016). Information flow and causality as rigorous notions ab initio. *Physical Review E*, 94(5), 052201. <https://doi.org/10.1103/PhysRevE.94.052201>

Louf, V., Jakob, C., Protat, A., Bergemann, M., & Narsey, S. (2019). The relationship of cloud number and size with their large-scale environment in deep tropical convection. *Geophysical Research Letters*, 46(15), 9203–9212. <https://doi.org/10.1029/2019GL083012>

Matsui, M., Michishita, K., & Yokoyama, S. (2020). Cloud-to-ground lightning flash density and the number of lightning flashes hitting wind turbines in Japan. *Electric Power Systems Research*, 181, 106066. <https://doi.org/10.1016/j.epsr.2020.106066>

Matthew, O. J., Abiye, O. E., & Ayoola, M. A. (2021). Assessment of static stability indices and related thermodynamic parameters for prediction of atmospheric convective potential and precipitation over Nigeria. *Meteorology and Atmospheric Physics*, 133(3), 675–691. <https://doi.org/10.1007/s00703-020-00758-9>

Oloketylui, J., & Omole, O. (2024). Investigating the influence of cosmic ray and solar activities on atmospheric weather dynamics within the equatorial electrojet region (Nigeria). *Discover Atmosphere*, 2, 5. <https://doi.org/10.1007/s44292-024-00006-6>

Peters, J. M., Chavas, D. R., Lebo, Z. J., & Su, C. Y. (2024). Cumulonimbus clouds convert a smaller fraction of CAPE into kinetic energy in a warmer atmosphere. *Journal of the Atmospheric Sciences*, 81(11), 1943–1961. <https://doi.org/10.1175/JAS-D-23-0107.1>

Pinto, P., & Belo-Pereira, M. (2020). Damaging convective and non-convective winds in southwestern Iberia during windstorm Xola. *Atmosphere*, 11, 692. <https://doi.org/10.3390/atmos11080692>

Sinclair, P. C., & Kuhn, P. M. (1991). Aircraft low-altitude wind shear detection and warning system. *Journal of Applied Meteorology and Climatology*, 30, 3–16.

Stips, A., Macias, D., Coughlan, C., Garcia-Gorriz, E., & Liang, X. S. (2016). *On the causal structure between CO₂ and global temperature*. *Scientific Reports*, 6, 21691. <https://doi.org/10.1038/srep21691>

Sun, W. Y., & Sun, O. M. (2019). Revisiting the parcel method and CAPE. *Dynamics of Atmospheres and Oceans*, 86, 134–152. <https://doi.org/10.1016/j.dynatmoce.2019.03.003>

Xu, K.-M., & Emanuel, K. A. (1989). Is the atmosphere conditionally unstable? *Journal of the Atmospheric Sciences*, 46(15), 2391–2403. [https://doi.org/10.1175/1520-0469\(1989\)046<2391:ITACU>2.0.CO;2](https://doi.org/10.1175/1520-0469(1989)046<2391:ITACU>2.0.CO;2)

Zeng, Z., Jin, G., Xu, C., Chen, S., & Zhang, L. (2022). Spacecraft telemetry anomaly detection based on parametric causality and double-criteria drift streaming peaks over threshold. *Applied Sciences*, 12(4), 1803. <https://doi.org/10.3390/app12041803>